

## VACCINES

# Long-term measles-induced immunomodulation increases overall childhood infectious disease mortality

Michael J. Mina,<sup>1,2\*</sup> C. Jessica E. Metcalf,<sup>1,3</sup> Rik L. de Swart,<sup>4</sup>  
A. D. M. E. Osterhaus,<sup>4</sup> Bryan T. Grenfell<sup>1,3</sup>

Immunosuppression after measles is known to predispose people to opportunistic infections for a period of several weeks to months. Using population-level data, we show that measles has a more prolonged effect on host resistance, extending over 2 to 3 years. We find that nonmeasles infectious disease mortality in high-income countries is tightly coupled to measles incidence at this lag, in both the pre- and post-vaccine eras. We conclude that long-term immunologic sequelae of measles drive interannual fluctuations in nonmeasles deaths. This is consistent with recent experimental work that attributes the immunosuppressive effects of measles to depletion of B and T lymphocytes. Our data provide an explanation for the long-term benefits of measles vaccination in preventing all-cause infectious disease. By preventing measles-associated immune memory loss, vaccination protects polymicrobial herd immunity.

Measles vaccines were introduced 50 years ago and were followed by striking reductions in child morbidity and mortality (1, 2). Measles control is now recognized as one of the most successful public health interventions ever undertaken (3). Despite this, in many countries vaccination targets remain unmet, and measles continues to take hundreds of thousands of lives each year (3). Even where control has been successful, vaccine hesitancy threatens the gains that have been made (1, 4). The introduction of mass measles vaccination has reduced childhood mortality by 30 to 50% in resource-poor countries (5–8) and by up to 90% in the most impoverished populations (9, 10). The observed benefits cannot be explained by the prevention of primary measles virus (MV) infections alone (11, 12), and they remain a central mystery (13).

MV infection is typified by a profound, but generally assumed to be transient, immunosuppression that renders hosts more susceptible to other pathogens (14–17). Thus, contemporaneous reductions in nonmeasles mortality after vaccination are expected. However, reductions in infectious disease mortality after measles vaccination can last throughout the first 5 years of life (5–10), which is much longer than anticipated by transient immunosuppression, which is generally considered to last for weeks to months (16, 17).

Proposed mechanisms for a nonspecific beneficial effect of measles vaccination range from suggestions that live vaccines may directly stimu-

late cross-reactive T cell responses or that they may train innate immunity to take on memory-like phenotypes (13, 18–21). Although well described by Aaby (11, 12) and others (22) in observational studies, primarily in low-resource settings, these effects may not fully explain the long-term benefits observed with measles vaccination and cannot explain the pre-vaccination associations of measles and infectious disease mortality we describe below. The World Health Organization (WHO) recently addressed this issue (22) and concluded that measles vaccination is associated with large reductions in all-cause childhood mortality but that there is no firm evidence to explain an immunological mechanism for the nonspecific vaccine benefits.

Recent work (17, 23) invoked a different hypothesis that a loss of immune memory cells after MV infection resets previously acquired immunity, and vaccination prevents this effect. de Vries *et al.* (17) reproduced transient measles immune suppression in macaques, characterized by systemic depletion of lymphocytes and reduced innate immune cell proliferation (24). Although peripheral blood lymphocyte counts were restored within weeks as expected (25), the authors hypothesized that rapid expansions of predominantly measles-specific B and T lymphocytes masked an ablated memory-cell population (17). In other words, MV infection replaced the previous memory cell repertoire with MV-specific lymphocytes, resulting in “immune amnesia” (17) to nonmeasles pathogens. Previous investigations of virus-induced memory-cell depletion suggest that recovery requires re-stimulation, either directly or via cross-reactive antigens (26–29).

We propose that, if loss of acquired immunological memory after measles exists, the resulting impaired host resistance should be detectable in the epidemiological data collected during periods when measles was common and [in contrast to

previous investigations that focus on low-resource settings (5–12)] should be apparent in high-resource settings where mortality from opportunistic infections during acute measles immune suppression was low. Relatively few countries report the necessary parallel measles and mortality time series to test this hypothesis. National-level data from England, Wales, the United States, and Denmark [Fig. 1, A to C; see supplementary materials (SM) 1 for details], spanning the decades surrounding the introduction of mass measles vaccination campaigns, meet our data criteria.

To assess the underlying immunological hypothesis (Fig. 1D) using population-level data, we required that first, nonmeasles mortality should be correlated with measles incidence data, especially because the onset of vaccination reduces the latter. Second, an immune memory loss mechanism should present as a strengthening of this association when measles incidence data are transformed to reflect an accumulation of previous measles cases (a measles “shadow”). For example, if immune memory loss (or more broadly, immunomodulation) lasts 3 years, the total number of immunomodulated individuals ( $S$ ) in the  $n$ th quarter can be calculated as the sum of the measles cases ( $M$ ) over the previous (and current) 12 quarters:  $S_n = M_{n-11} + M_{n-10} + \dots + M_{n-1} + M_n$ . In practice, we weighted the quarters using a gamma function. Dividing  $S$  by the total population of interest thus provides the prevalence of immunomodulation (see SM 2, and 3; fig. S1, A to C; and movie S1 for detailed methods). Third, the strength of this association should be greatest when the mean duration over which the cases are accumulated matches the mean duration required to restore immunological memory after MV infection. Fourth, the estimated duration should be consistent both with the available evidence of increased risk of mortality after MV, compared with uninfected children, and with the time required to build a protective immune repertoire in early life (Fig. 1D, fig. S2, and SM 5 and 6).

To explicitly address whether the observed nonspecific benefits of vaccination can be attributed to the prevention of MV immunomodulation, evidence for the four hypotheses must be present separately within the pre-vaccine eras.

Reductions in nonmeasles infectious disease mortality (SM 1) are shown in Fig. 1, for children aged 1 to 9 years in Europe and aged 1 to 14 years in the United States, shortly after the onset of mass vaccination in each country. The fall in mortality was later in Denmark, corresponding to the introduction of measles vaccination in the 1980s, as compared to the late 1960s for the United Kingdom and United States. In all locations, measles incidence showed significant ( $P < 0.001$ ) associations with mortality (Fig. 1, E to G). However, effect sizes varied (fig. S3A), reflecting low reporting in the United States [fig. S3B and (30)] and changes in health care practice between eras. Adjusting for year as a covariate (SM 4) had little effect on the point estimates (fig. S3C). These associations could reflect transient measles immune suppression. Thus, to address our second hypothesis that MV immunomodulation can explain

<sup>1</sup>Department of Ecology and Evolutionary Biology, Princeton University, Princeton, NJ, USA. <sup>2</sup>Medical Scientist Training Program, School of Medicine, Emory University, Atlanta, GA, USA. <sup>3</sup>Fogarty International Center, National Institutes of Health, Bethesda, MD, USA. <sup>4</sup>Department of Viroscience, Erasmus University Medical Center, Rotterdam, Netherlands.  
\*Corresponding author. E-mail: michael.j.mina@gmail.com

long-term increased mortality and, consequently, improved survival after vaccination, we transformed measles incidence into population prevalence of MV immunomodulation, with the duration of the immunomodulation (the time required to rebuild sufficiently protective immune memory) defined by a gamma distribution to weight the previous time points summed together, as discussed above and in SM 2 and movie S1.

When the gamma-distributed transformation was applied to the England and Wales measles data, the best-fit duration of MV immunomodulation, as determined by the linear fit of the corresponding prevalence of MV immunomodulation to the mortality data (SM 3), centered at a 28.3-month duration of measles-induced immunomodulation. This corresponded to a strong and significantly improved association between mea-

les and all-cause infectious disease mortality [coefficient of determination ( $R^2$ ) = 0.92 versus 0.37;  $P < 0.00001$ ; Fig. 2, A to C]. Simpler additive transformations (SM 2 and movie S1) return the same qualitative pattern (Fig. 2D), and adjusting for year in the model had no effect (fig. S4). Figure 2, E and F, shows the time series for the actual and predicted mortalities (calculated from the linear fits), together with the prevalence of

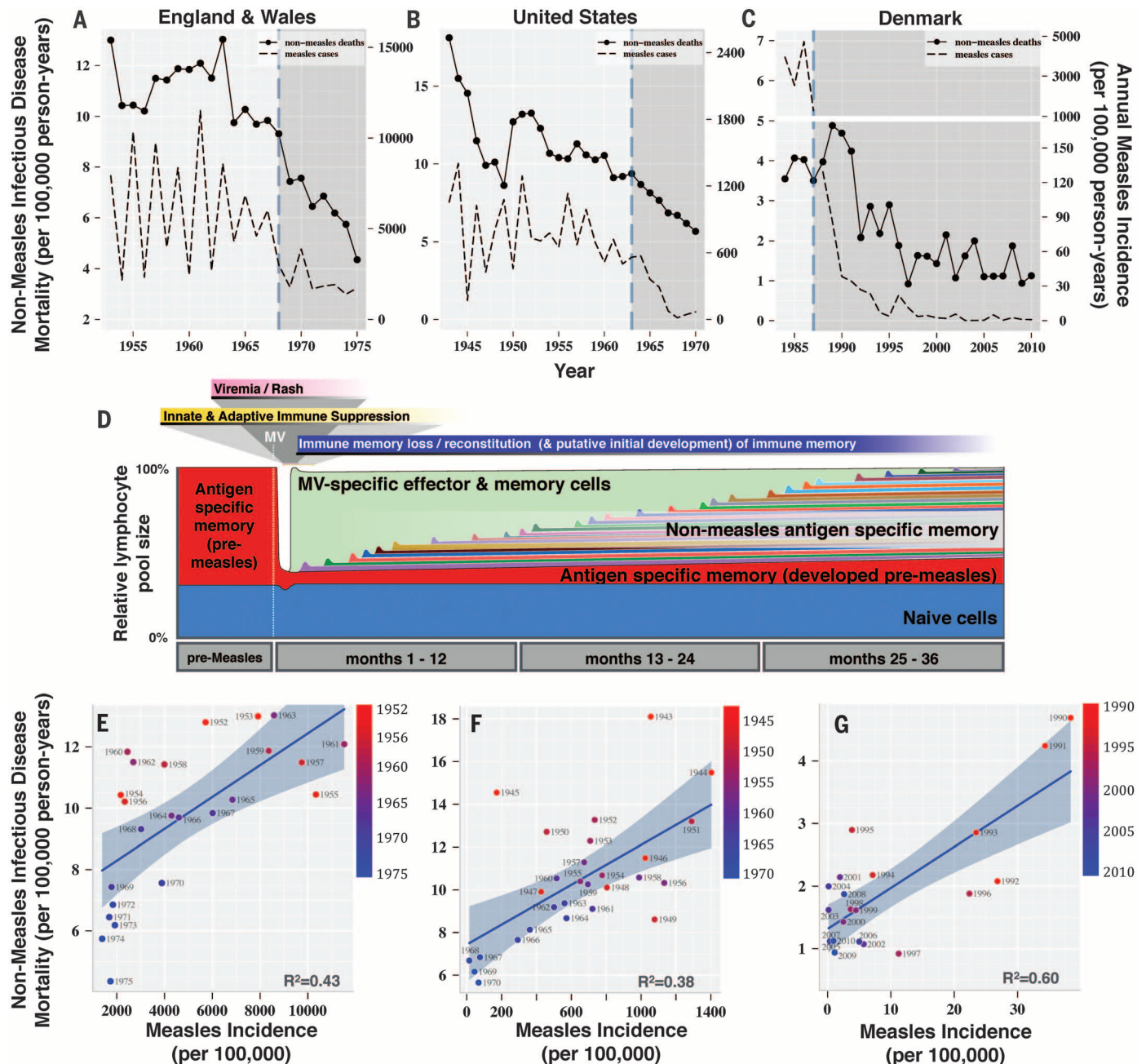


**Fig. 1. Measles incidence, nonmeasles infectious disease mortality, and measles-induced immunomodulation.** Nonmeasles infectious disease mortality and measles incidence time series (A to C) and regressions (E to G) are shown for England and Wales, the United States, and Denmark. The vertical dashed lines in (A) to (C) indicate the year of introduction of the measles vaccine. (D) Measles-induced lymphopenia and subsequent measles-specific lymphocyte expansion in

the weeks after MV infection, as described in (17, 23), are shown, and time is extended to depict hypothesized long-term immunomodulatory effects of MV infection and reconstitution of the immune response through individual exposures. Scatter plots and best-fit regression curves (plotted with 95% confidence bands) are shown for nonmeasles infectious disease mortality versus measles incidence for England and Wales (E), the United States (F), and Denmark (G).

MV immunomodulation (see movie S2 for the full paths of these transformations). Overall, a simple weighted integral of measles incidence captures the nonmeasles mortality data remarkably well and more closely than the raw incidence.

To evaluate our fourth hypothesis, we compared the best-fit gamma distribution (indicating average time to return of full immunity) to (i) the previously observed (31) duration of elevated relative risk (RR) of all-cause mortality after intensive measles exposure (albeit in children exposed before 6 months of age) and (ii) to the global age distribution (fig. S2) of bacterial invasive disease

in children under 5 years of age [an estimate for the time required to build protective immunity (32)]. Both the elevated RR of mortality after measles exposure and declines from peak rates of bacterial disease, indicating the development of sufficiently protective immunity, fell precisely along the gamma curve ( $R^2 = 0.97$  and  $0.99$ , respectively; Fig. 2G).

We tested these results for nonspecific effects of vaccination (II) by applying the same procedure to the pre-vaccination data alone. Before vaccination, the best-fit duration of MV immunomodulation was no different (centered at 28.0

versus 28.3 months; Fig. 2, B to D, and fig. S5A) and closely matched the duration identified in the post-vaccine era as well (29.2 months; fig. S5A). Moreover, the coefficients describing the slope of mortality rate versus prevalence of immunomodulation were nearly identical (Fig. 2, B and I, and fig. S5B). This effect held regardless of which era's respective best-fit gamma transform was used (fig. S5, B to D), because optimizing the transformation using only the pre-vaccine data permitted accurate prediction of the post-vaccine era data that was not used to fit the model (known as out-of-sample prediction). The results

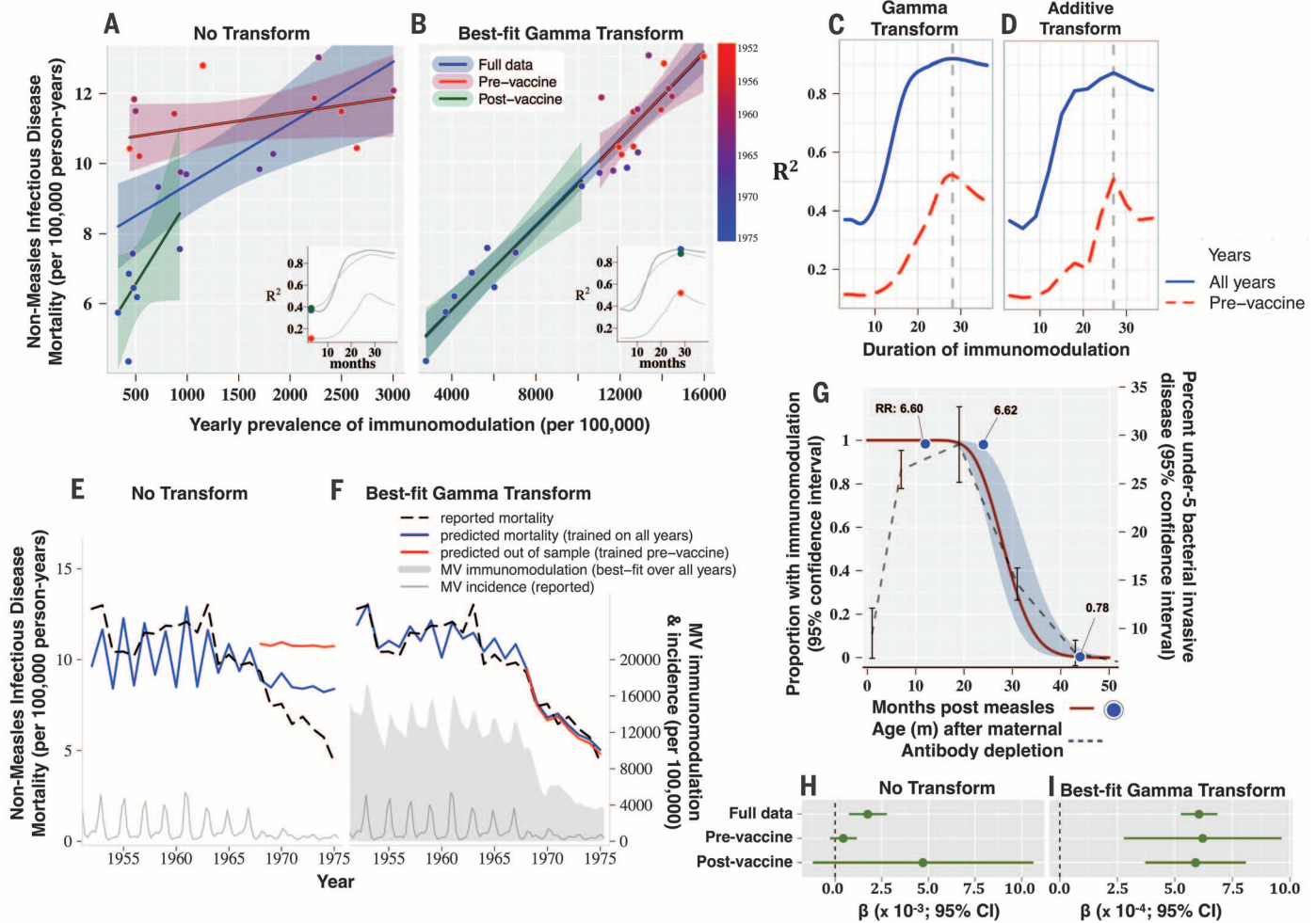


**Fig. 2. England and Wales: Measles-induced immunomodulation and nonmeasles infectious disease mortality (1952–1975).** Annual incidence of nonmeasles infectious disease mortality regressed against the prevalence of MV immunomodulation, given (A) no transform or (B) the best-fit gamma transform (that provides the best linear fit,  $R^2$ , to the data). Individual regression lines and 95% confidence intervals are plotted for regressions over the full data set (blue), the pre-vaccine era data only (green), and the post-vaccine era data only (red).  $R^2$  is plotted against the mean duration of MV immunomodulation for the (C) gamma or (D) additive transformation for the full data set (blue lines) or the pre-vaccine data only (red lines). Inset graphs in (A) and (B) are the same as (C), and the location of the dots (color coded as per the regression lines) represent the duration of immunomodulation and the  $R^2$  values associated with the scatter plot shown. In (E and F), the measured nonmeasles infectious disease mortality is plotted (broken line) along with the predicted annual mortalities (solid blue and red lines), predicted using the

regression coefficients from the (H) untransformed or (I) best-fit transformed data. Predictions in (E) and (F) are either in sample and based on the full data set (blue line), or out of sample and based on the pre-vaccine data only (red line). In (F), for example, the in-sample mortality prediction is made from the regression coefficients (I) from the best-fit transformed data for the full data set (blue line), and mortality is also predicted entirely out of sample for the post-vaccine era by optimizing the gamma transformation and calculating regression coefficients using only data from the pre-vaccine era (red line; fig. S5C). (G) The best-fit gamma distribution (optimized against the full data set) is shown (dark red line), along with the distribution of under-5 bacterial invasive disease versus age after the depletion of maternal antibodies (broken gray line), and the relative risk of non-MV mortality after MV infection, described in (31), is also shown plotted against time since MV infection (blue points). (H) and (I) The regression coefficients for the best-fit lines shown in (A) and (B) are plotted with 95% confidence intervals in (H) and (I), respectively.

are robust to the chosen focal age groups (1 to 4 and 5 to 9 years old age groups shown in fig. S6) and are sensitive to the specific order and magnitude of the measles epidemics, because randomizing the time series by year erased the above effects (fig. S7).

Furthermore, results were robust to individual disease classes (table S1), with best-fit durations of immunomodulation predisposing to individual classes of infectious disease mortality lasting between 18 and 30 months (mean, 27 months; median, 24 months). Exceptions were rubella [although rubella was not included in the primary analysis (SM 1)] and septicemia, which had best-fit durations of immune memory loss of approximately 12 and 3 months, respectively.

Many previous investigations described stronger nonspecific benefits of MV vaccination in females than males (7, 11, 13); thus, as an additional test of our hypotheses, we also compared genders. In agreement, we found consistently stronger associations among females (fig. S8). To test the England and Wales findings, we applied the full analysis to data from the United States (Fig. 3 and movie S3). Here, the optimized gamma transformation centered at 30.9 months (versus 28.3

for the United Kingdom) again greatly improved the fit of the data ( $R^2 = 0.88$  versus 0.42; Fig. 3, A to F), showed very strong agreement with previously observed durations of mortality risk after intensive measles exposure ( $R^2 = 0.999$ , Fig. 3G), and was predicted by the age distribution of invasive bacterial infections in children under 5 ( $R^2 = 0.921$ ; Fig. 3G).

We tested whether declines in mortality after vaccination were caused by nonspecific benefits of vaccination. Transformation of the data from the pre-vaccine era increased the strength of the association markedly ( $R^2 = 0.87$  versus 0.07). As in the United Kingdom, very similar best-fit gamma transformations were obtained before (and after) vaccination (centered at 30.3 and 29.2 months; Fig. 3C and fig. S9A); the coefficients of association (with mortality) across vaccine eras were again consistent (Fig. 3, B and I, and fig. S9); the results were robust across age groups (fig. S10); the strengths of association were stronger in females (fig. S11); and adjusting for year had no effect (fig. S12).

The data from Denmark (SM 1) were recorded at yearly rather than quarterly intervals and limited the scope of analyses. Furthermore, because

measles vaccine introduction in Denmark in 1987 occurred as data became available and was so successful that within its first year, measles incidence was reduced by an order of magnitude (Fig. 1C), we were compelled to focus on the two decades that followed the logarithmic reduction of cases (1990–2010). Despite these limitations, transformation of the yearly data (using eqs. 3 and 8 in SM 2) led to steep peaks in model fit at 30 months duration of MV immunomodulation that predicted mortality ( $R^2 = 0.77$ ; Fig. 4A). When we inferred quarterly incidence data from the annualized data [using monthly measles incidence data from a large population sample in Denmark (33) to estimate proportions of annual cases occurring each quarter; SM 1], the best fit indicated a 26.4-month duration of MV immunomodulation (Fig. 4, B and E), agreeing with the durations defined for England and Wales and the United States above, as well as the previously observed risk of mortality after measles (Fig. 4C).

These results provide population evidence for a generalized prolonged (roughly 2- to 3-year) impact of measles infection on subsequent mortality from other infectious diseases. Fluctuations

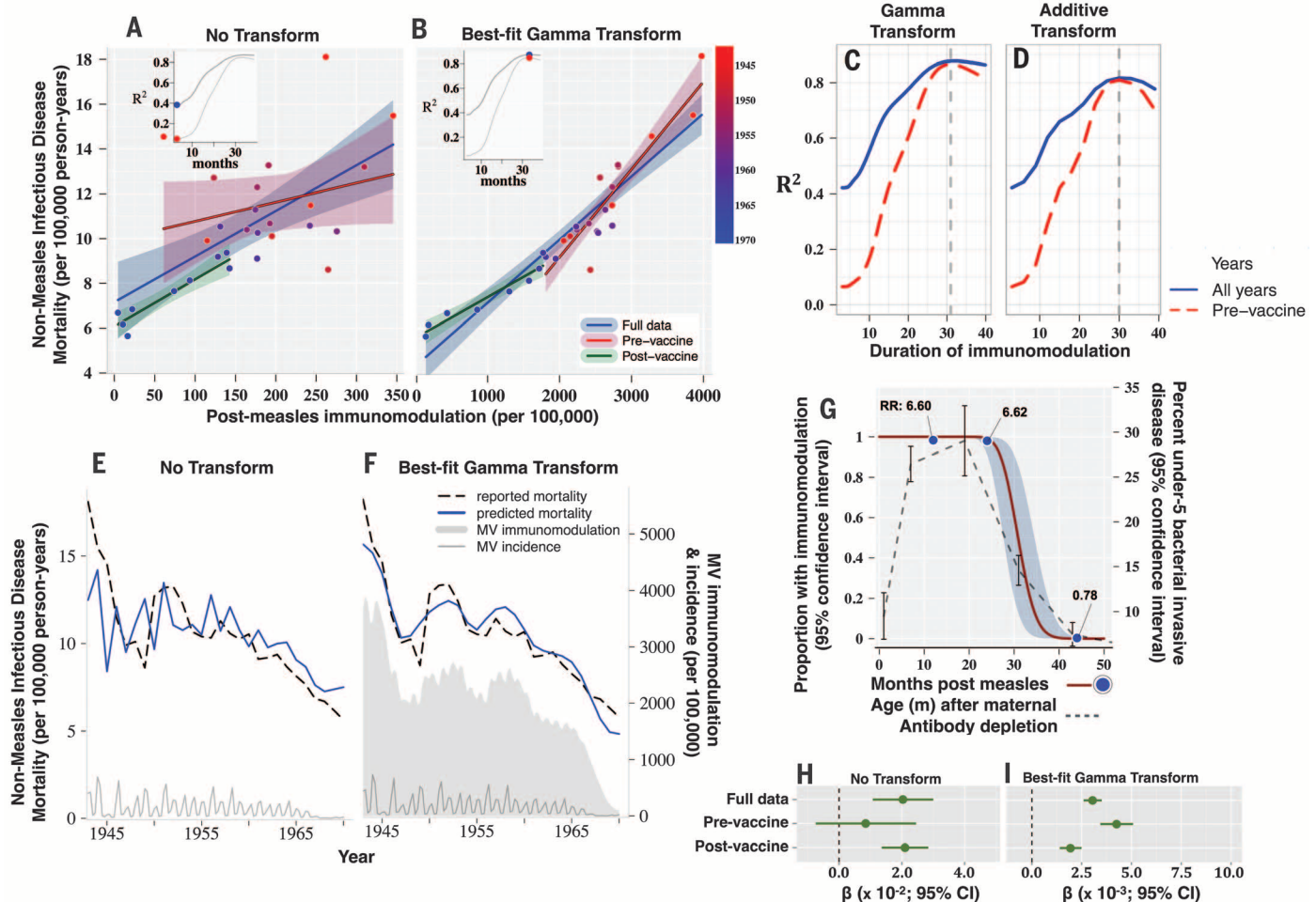


**Fig. 3. USA: Measles-induced immunomodulation and nonmeasles infectious disease mortality (1943–1970).** (A to I) Plots are as described for England and Wales in Fig. 2.

in childhood mortality in the United Kingdom, the United States, and Denmark are explained by a simple weighted integral that describes the prevalence of measles immune memory loss and thus captures the impact of measles infection and immune depletion. We anticipate that morbidity data might show stronger effects.

As a further test of the immunosuppressive impact of measles, we carried out a similar analysis on pertussis. Pertussis is a vaccine-preventable disease that is not known to be immunosuppressive and for which high-quality weekly data (34) are available for England and Wales that were collected during the pre-measles vaccine years described above. We found no correlation (fig. S13) between pertussis incidence and non-pertussis infectious disease mortality. No correlation was observed even when the pertussis data were transformed to reflect the sum of previous pertussis cases (a pertussis “shadow”) extending over 48 months (fig. S13).

Our results show that when measles was common, MV infections could have been implicated in as many as half of all childhood deaths from infectious disease, thus accounting for nearly all of the interannual fluctuations in childhood infectious disease deaths. The reduction of MV in-

fections was the main factor in reducing overall childhood infectious disease mortality after the introduction of vaccination.

Consistency in the best-fit duration of MV immunomodulation (the time required to restore protective immune memory) in all three countries, the close fit to observed durations of increased mortality after intensive MV exposure, and its correspondence to the early development of immunity (before 5 years of age) through exposure all provide strong evidence for a measles immune effect. The similarity in results obtained for both pre- and post-vaccine eras, the qualitative consistency across ages, and the stronger associations in females (7) provide further support for an underlying immunomodulatory mechanism. Finally, these results are consistent with multiple immuno-epidemiologic and case-controlled studies that show reduced or absent antigen-specific cellular responses lasting 3 years after measles (35, 36) and reduced atopy even 15 years after infection (37).

The correspondence between our results and previous epidemiological data by Aaby *et al.* (31) should be viewed with the caveat that the increased relative risk of mortality after intensive measles exposure was measured in children ex-

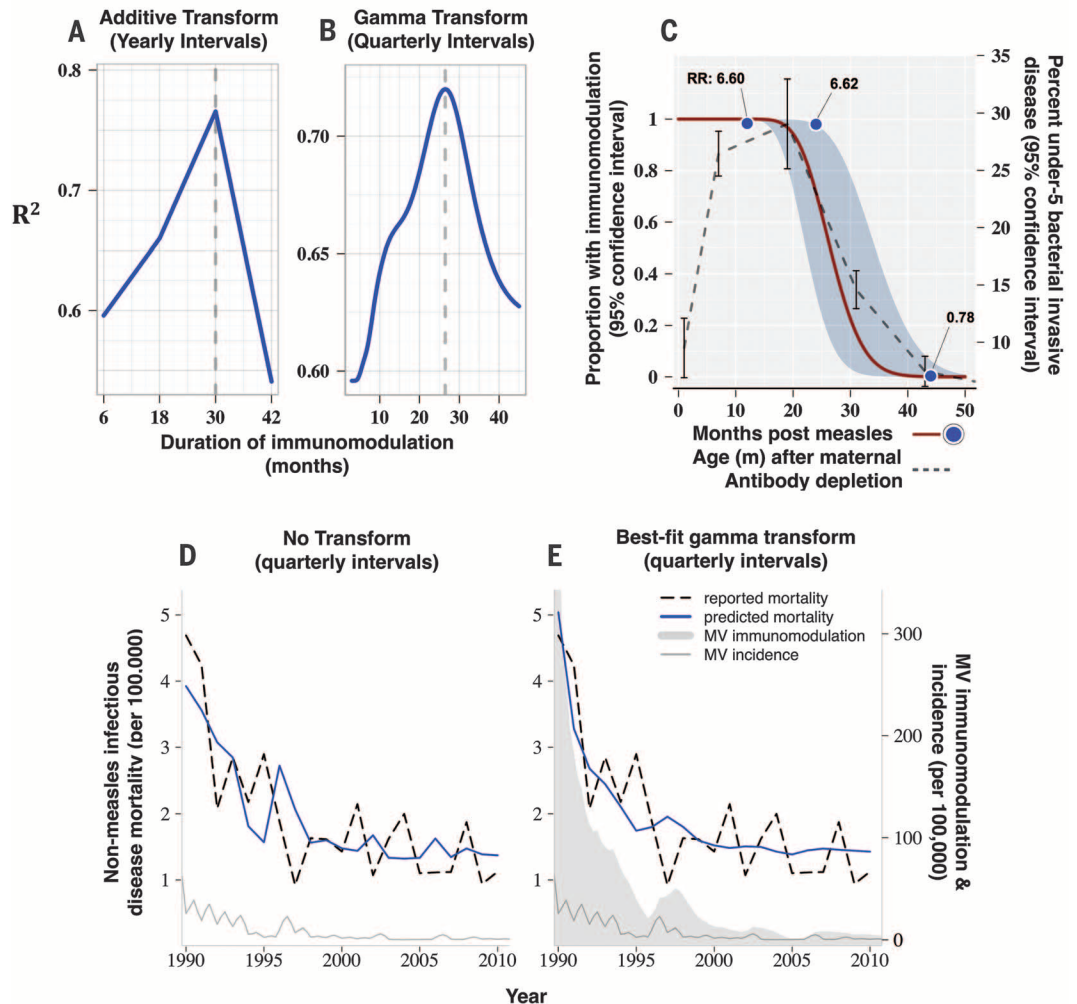
posed before 6 months of age, not all of whom developed features of clinical measles infections. Other studies (12, 38, 39) have failed to detect long-term immunologic sequelae of measles. These previous cohort studies have focused on low-income countries, primarily in West Africa, where very high rates of death from opportunistic infections during acute measles immune suppression drive mortality dynamics and mask the pernicious long-term immunological effects of measles infection. For example, approximately 50% of all childhood deaths recorded over 5 years of follow-up occurred within only 2 months of measles infection, precluding the detection of long-term sequelae in those children.

MV infection and vaccination produce strong and durable herd immunity against subsequent epidemics (40). Our results thus suggest an extra dynamical twist: MV infections could also reduce population immunity against other infections in which MV immunomodulation could be envisioned as a measles-induced immune amnesia (17); hence, measles vaccination might also be preserving herd protection against nonmeasles infections.

Measles vaccination is one of the most cost-effective interventions for global health, and our results imply further immunological dividends:

**Fig. 4. Denmark: Measles-induced immunomodulation and non-MV infectious disease mortality (1990–2010).**

$R^2$  versus duration of measles-induced immunomodulation when measles data are transformed using (A) the additive transformation with yearly intervals or (B) the gamma transform with quarterly intervals, where yearly measles incidence was converted to quarterly incidence based on (33). The best-fit gamma transform (C), as well as the predicted nonmeasles mortality, predicted from the untransformed (D) or the best-fit gamma transform (E) MV immunomodulation data, are shown and are described for the respective figures in Figs. 2 and 3.



mortality (and probably morbidity) reductions linked to measles vaccination might be much greater than previously considered. This is of particular importance today where, especially in wealthy nations, reduced opportunistic infections during acute measles immunosuppression, added to the comparative rarity of infection, has led to a public view of measles as a benign childhood disease. Our findings help dispel the mystery surrounding the disproportionately large reductions in mortality seen after the introduction of measles vaccinations and reinforce the importance of measles vaccination in a global context.

## REFERENCES AND NOTES

- W. J. Moss, D. E. Griffin, *Lancet* **379**, 153–164 (2012).
- E. Simons *et al.*, *Lancet* **379**, 2173–2178 (2012).
- R. T. Perry *et al.*, *MMWR Morb. Mortal. Wkly. Rep.* **63**, 103–107 (2014).
- S. B. Omer, D. A. Salmon, W. A. Orenstein, M. P. deHart, N. Halsey, *N. Engl. J. Med.* **360**, 1981–1988 (2009).
- J. D. Clemens *et al.*, *Am. J. Epidemiol.* **128**, 1330–1339 (1988).
- M. A. Koenig *et al.*, *Bull. World Health Organ.* **68**, 441–447 (1990).
- A. Desgrées du Loué, G. Pison, P. Aaby, *Am. J. Epidemiol.* **142**, 643–652 (1995).
- P. Aaby, J. Bukh, I. M. Lisse, A. J. Smits, *J. Infect.* **8**, 13–21 (1984).
- E. A. Holt, R. Boulos, N. A. Halsey, L. M. Boulos, C. Boulos, *Pediatrics* **85**, 188–194 (1990).
- Z. Kabir, J. Long, V. P. Reddaiah, J. Kevany, S. K. Kapoor, *Bull. World Health Organ.* **81**, 244–250 (2003).
- P. Aaby, T. R. Kollmann, C. S. Benn, *Nat. Immunol.* **15**, 895–899 (2014).
- P. Aaby *et al.*, *Int. J. Epidemiol.* **32**, 106–115 (2003).
- K. L. Flanagan *et al.*, *Clin. Infect. Dis.* **57**, 283–289 (2013).
- C. L. Karp *et al.*, *Science* **273**, 228–231 (1996).
- B. Hahm, *Curr. Top. Microbiol. Immunol.* **330**, 271–287 (2009).
- S. Schneider-Schaulies, J. Schneider-Schaulies, *Curr. Top. Microbiol. Immunol.* **330**, 243–269 (2009).
- R. D. de Vries *et al.*, *PLoS Pathog.* **8**, e1002885 (2012).
- J. Kleijnenhuis *et al.*, *Proc. Natl. Acad. Sci. U.S.A.* **109**, 17537–17542 (2012).
- G. R. Lee, S. T. Kim, C. G. Spilianakis, P. E. Fields, R. A. Flavell, *Immunity* **24**, 369–379 (2006).
- M. G. Netea, J. Quintin, J. W. van der Meer, *Cell Host Microbe* **9**, 355–361 (2011).
- S. Saeed *et al.*, *Science* **345**, 1251086 (2014).
- WHO, Meeting of the Strategic Advisory Group of Experts on immunization, March 2014, *Systematic Review of the Non-specific Effects of BCG, DTP and Measles Containing Vaccines*, [http://www.who.int/immunization/sage/meetings/2014/april/3\\_NSE\\_Epidemiology\\_review\\_Report\\_to\\_SAGE\\_14\\_Mar\\_FINAL.pdf](http://www.who.int/immunization/sage/meetings/2014/april/3_NSE_Epidemiology_review_Report_to_SAGE_14_Mar_FINAL.pdf).
- R. D. de Vries, R. L. de Swart, *PLoS Pathog.* **10**, e1004482 (2014).
- W. H. Lin, R. D. Kouyos, R. J. Adams, B. T. Grenfell, D. E. Griffin, *Proc. Natl. Acad. Sci. U.S.A.* **109**, 14989–14994 (2012).
- R. T. Perry, N. A. Halsey, *J. Infect. Dis.* **189**, S4–S16 (2004).
- L. K. Selin, K. Vergilis, R. M. Welsh, S. R. Nahill, *J. Exp. Med.* **183**, 2489–2499 (1996).
- S. K. Kim, M. A. Brehm, R. M. Welsh, L. K. Selin, *J. Immunol.* **169**, 90–98 (2002).
- S. K. Kim, R. M. Welsh, *J. Immunol.* **172**, 3139–3150 (2004).
- C. D. Peacock, S. K. Kim, R. M. Welsh, *J. Immunol.* **171**, 655–663 (2003).
- A. R. Hinman, W. A. Orenstein, M. J. Papania, *J. Infect. Dis.* **189**, S17–S22 (2004).
- P. Aaby, J. Bukh, D. Kronborg, I. M. Lisse, M. C. da Silva, *Am. J. Epidemiol.* **132**, 211–219 (1990).
- WHO, *Global Review of the Distribution of Pneumococcal Invasive Disease by Age and Region* (2011); [www.who.int/immunization/sage/6\\_Russel\\_review\\_age\\_specific\\_epidemiology\\_PCV\\_schedules\\_session\\_nov11.pdf](http://www.who.int/immunization/sage/6_Russel_review_age_specific_epidemiology_PCV_schedules_session_nov11.pdf).
- O. Horwitz, K. Grünfeld, B. Lysgaard-Hansen, K. Kjeldsen, *Am. J. Epidemiol.* **100**, 136–149 (1974).
- J. A. Clarkson, P. E. M. Fine, *Int. J. Epidemiol.* **14**, 153–168 (1985).
- A. Kipps, L. Stern, E. Vaughan, *S. Afr. Med. J.* **86**, 104–108 (1996).
- S. O. Shaheen *et al.*, *BMJ* **313**, 969–974 (1996).
- S. O. Shaheen *et al.*, *Lancet* **347**, 1792–1796 (1996).
- P. Aaby, B. Samb, M. Andersen, F. Simondon, *Am. J. Epidemiol.* **143**, 1035–1041 (1996).
- P. Aaby, I. M. Lisse, K. Mølbak, K. Knudsen, H. Whittle, *Pediatr. Infect. Dis. J.* **15**, 39–44 (1996).
- D. J. Earn, P. Rohani, B. M. Bolker, B. T. Grenfell, *Science* **287**, 667–670 (2000).

## ACKNOWLEDGMENTS

Data for analyses regarding England and Wales were retrieved from the Office of Population Censuses and Surveys and the Office for National Statistics ([www.ons.gov.uk](http://www.ons.gov.uk)). We thank P. Rohani for supplying us with historical data on pertussis, as originally described in (34). Data for U.S. analyses were retrieved from the U.S. Centers for Disease Control and Prevention, National Center for Health Statistics ([www.cdc.gov/nchs](http://www.cdc.gov/nchs)). Data for Denmark was retrieved from Statistics Denmark ([www.statbank.dk](http://www.statbank.dk)) and WHO ([www.apps.who.int](http://www.apps.who.int)). This work is funded by the Bill and Melinda

Gates Foundation, the Science and Technology Directorate of the Department of Homeland Security [contract HSHQDC-12-C-00058 (B.T.G. and C.J.E.M.)], and the RAPIDD program of the Science and Technology Directorate of the Department of Homeland Security and the Fogarty International Center, National Institutes of Health (C.J.E.M. and B.T.G.).

## SUPPLEMENTARY MATERIALS

[www.sciencemag.org/content/348/6235/694/suppl/DC1](http://www.sciencemag.org/content/348/6235/694/suppl/DC1)

Materials and Methods  
Supplementary Text  
Figs. S1 to S13  
Table S1  
References (41–43)  
Movies S1 to S3

24 November 2014; accepted 1 April 2015  
10.1126/science.aaa3662

## CHROMOSOMES

# CENP-C reshapes and stabilizes CENP-A nucleosomes at the centromere

Samantha J. Falk,<sup>1,2\*</sup> Lucie Y. Guo,<sup>1,3\*</sup> Nikolina Sekulic,<sup>1\*</sup> Evan M. Smoak,<sup>1,3,4\*</sup> Tomoyasu Mani,<sup>1,3</sup> Glennis A. Logsdon,<sup>1,3</sup> Kushol Gupta,<sup>1</sup> Lars E. T. Jansen,<sup>5</sup> Gregory D. Van Duyne,<sup>1,3</sup> Sergei A. Vinogradov,<sup>1,3</sup> Michael A. Lampson,<sup>2,3,4</sup> Ben E. Black<sup>1,2,3,†</sup>

**Inheritance of each chromosome depends upon its centromere. A histone H3 variant, centromere protein A (CENP-A), is essential for epigenetically marking centromere location. We find that CENP-A is quantitatively retained at the centromere upon which it is initially assembled. CENP-C binds to CENP-A nucleosomes and is a prime candidate to stabilize centromeric chromatin. Using purified components, we find that CENP-C reshapes the octameric histone core of CENP-A nucleosomes, rigidifies both surface and internal nucleosome structure, and modulates terminal DNA to match the loose wrap that is found on native CENP-A nucleosomes at functional human centromeres. Thus, CENP-C affects nucleosome shape and dynamics in a manner analogous to allosteric regulation of enzymes. CENP-C depletion leads to rapid removal of CENP-A from centromeres, indicating their collaboration in maintaining centromere identity.**

**C**entromeres direct chromosome inheritance at cell division, and nucleosomes containing a histone H3 variant, centromere protein A (CENP-A), are central to current models of an epigenetic program for specifying centromere location (1). The centromere inheritance model in metazoans suggests that the high local concentration of preexisting CENP-A nucleosomes at the centromere guides the assembly of nascent

CENP-A, which occurs once per cell cycle after mitotic exit. This model predicts that after initial assembly into centromeric chromatin, CENP-A must be stably retained at that centromere; otherwise, centromere identity would be lost before the next opportunity for new loading in the next cell cycle. Here, we use biochemical reconstitution to measure the shape and physical properties of CENP-A nucleosomes with and without its close binding partner, CENP-C, and combine these studies with functional tests that reveal the mechanisms underlying the high stability of centromeric chromatin.

CENP-C recognizes CENP-A nucleosomes via a region termed its central domain (amino acids 426 to 537; CENP-C<sup>CD</sup>) (2, 3). We first considered how CENP-C<sup>CD</sup> may affect the overall shape of the CENP-A-containing nucleosome using an intranucleosomal fluorescence resonance energy transfer (FRET)-based approach. We designed an experiment to measure FRET efficiency,  $\Phi_{\text{FRET}}$ ,

<sup>1</sup>Department of Biochemistry and Biophysics, Perelman School of Medicine, University of Pennsylvania, Philadelphia, PA 19104, USA. <sup>2</sup>Graduate Program in Cell and Molecular Biology, Perelman School of Medicine, University of Pennsylvania, Philadelphia, PA 19104, USA. <sup>3</sup>Graduate Program in Biochemistry and Molecular Biophysics, Perelman School of Medicine, University of Pennsylvania, Philadelphia, PA 19104, USA. <sup>4</sup>Department of Biology, University of Pennsylvania, Philadelphia, PA 19104, USA. <sup>5</sup>Instituto Gulbenkian de Ciência, 2780-156 Oeiras, Portugal. \*These authors contributed equally to this work. †Corresponding author. E-mail: blackbe@mail.med.upenn.edu

---

*This copy is for your personal, non-commercial use only.*

---

**If you wish to distribute this article to others**, you can order high-quality copies for your colleagues, clients, or customers by [clicking here](#).

**Permission to republish or repurpose articles or portions of articles** can be obtained by following the guidelines [here](#).

**The following resources related to this article are available online at [www.sciencemag.org](http://www.sciencemag.org) (this information is current as of May 7, 2015):**

**Updated information and services**, including high-resolution figures, can be found in the online version of this article at:

<http://www.sciencemag.org/content/348/6235/694.full.html>

**Supporting Online Material** can be found at:

<http://www.sciencemag.org/content/suppl/2015/05/06/348.6235.694.DC1.html>

A list of selected additional articles on the Science Web sites **related to this article** can be found at:

<http://www.sciencemag.org/content/348/6235/694.full.html#related>

This article **cites 41 articles**, 22 of which can be accessed free:

<http://www.sciencemag.org/content/348/6235/694.full.html#ref-list-1>

This article appears in the following **subject collections**:

Medicine, Diseases

<http://www.sciencemag.org/cgi/collection/medicine>